Dispersive electron transport in polycrystalline films of CdTe

R. Ramírez-Bon
Centro de Investigación en Física, Universidad de Sonora, Apartado Postal 5-88, Hermosillo, Sonora 83190, Mexico

F. Sánchez-Sinencio, G. González de la Cruz, and O. Zelaya
Departamento de Física, Centro de Investigación y de Estudios Avanzados del Instituto Politécnico Nacional, Apartado Postal 14-740, 0700 México, Distrito Federal, Mexico

(Received 3 December 1992; revised manuscript received 5 March 1993)

Electron transient transport has been studied in CdTe polycrystallilne films by means of the time-of-flight technique. The samples studied were intrinsic CdTe polycrystalline films with a grain size from about 100 nm to 20 μm. The transit time was measured in the largest-grain-size films. The transient transport has the characteristics of dispersive transient transport as observed in disordered materials such as amorphous semiconductors, glasses, etc. For the smaller-grain-size films it is not possible to determine a transit time in the photocurrent traces, due to the effects of recombination and deep trapping of charge. However, the transport characterization allows the determination of the dispersive nature of the electron transport in these films. In addition, in one kind of these smaller-grain-size films, it was possible to identify the presence of a localized state as being responsible for the photocurrent peak exhibited in the photocurrent traces. This peak is explained by a multiple-trapping model with a single-trapping level along with a recombination center.

I. INTRODUCTION

Electronic transient transport has been extensively studied in single crystalline[1] and disordered materials,[2–5] however it is only recently that electronic transient transport measurements in polycrystalline semiconductors have been reported.[6,7] In most of the cases of single crystalline materials the observed transient transport corresponds to Gaussian transport, while in the case of disordered solids the reported transport has the characteristics of non-Gaussian transport. Considering that polycrystalline semiconductors are intermediate between the above two cases, it seems important to investigate the basic properties of the transient transport through these materials. Polycrystalline systems are composed of a great number of small crystallites. The main feature of these systems come from the bulk and grain boundaries of the crystallites.

Electrical transport phenomena through the grain boundaries of polycrystalline semiconductors have been mainly studied by steady-state techniques.[8] For intrinsic polycrystalline semiconductors with high resistivity, these techniques present a severe problem due to the necessity of Ohmic contacts for the electrical measurements. On the other hand, transient techniques for the study of charge-carrier transport provide a method for determining some important characteristics such as charge-carrier drift mobility, lifetime, trapping parameters, etc.[1,4,5] The importance of these techniques increases when they are applied to high-resistivity materials, because contact Ohmicity is not necessary. Electrical transport through the grain boundaries of high-resistivity polycrystalline material like intrinsic CdTe can be better understood by applying these techniques. In this work we have studied the electron transient transport in intrinsic CdTe polycrystalline films. This study was performed by measuring transient photocurrent between coplanar electrodes on the films, using the time-of-flight (TOF) technique. Three kinds of film were studied: films having grain size about 20 μm grown by close-spaced vapor transport (CSVT) and films with a smaller grain size (about 100 nm) grown by hot-wall-flash evaporation (HWFE) or by rf sputtering techniques. The experimental results for the transient transport and a discussion are presented in Sec. III for each of the different kinds of film.

For the largest-grain-size films, it was possible to measure a transit time in the photocurrent traces. It was seen that the photocurrent shape has a power-law behavior as observed in disordered materials. The general characteristics of the electronic transport in these films correspond to those of the dispersive transient transport. The dispersion observed is explained in terms of a wide energy distribution of the defects in the films, both in the bulk grain material and in the grain boundaries.[6] The smaller-grain-size films exhibit a greater influence of deep trapping and recombination of charge, which do not allow a transit-time determination. The transient transport also has the characteristics of dispersive transport. The occurrence of deep trapping and recombination of charge is explained by the influence on the electron transport of the greater number per unit length of grain boundaries in these films. In the films grown by the HWFE technique, the transient photocurrents also exhibit a photocurrent peak, with a position in time which is very sensitive to temperature. This peak is explained by the presence of a localized trapping center in the energy band gap of these films. It is found that a multiple-trapping model with a single trapping level, along with a recombination center, is appropriate to describe the photocurrent peak observed in these films.[7]

0163-1829/93/48(4)/2200(7)/$06.00 ©1993 The American Physical Society

II. EXPERIMENTAL DETAILS

The samples studied are CdTe polycrystalline films grown on 7059 Corning glass substrates by the close-spaced vapor transport, hot-wall-flash evaporation, and rf sputtering techniques. The films grown by the CSVT technique have dimensions 2 cm×1 cm×20–100 μm, with a typical grain size about 20 μm. This grain size is obtained with typical growth conditions of 1.5 mTorr of argon pressure and 650 °C and 550 °C for the temperatures of source and substrate, respectively. The dimensions of the films grown by the HWFE technique are 2 cm×1 cm×150–250 nm, with a typical average grain size about 100 nm, obtained by using a substrate temperature of 250 °C during the growth. The rf sputtered films have dimensions and grain size similar to the films grown by the HWFE technique. The typical growth conditions for these films were room temperature for the substrate and 10^{-2} Torr for the argon pressure. The polycrystalline character of the films is shown by x-ray-diffraction measurements of the films, which display the CdTe cubic phase pattern. This pattern also shows a slight preferred orientation along the (111) direction.

The charge-carrier transient transport was studied by measuring transient photocurrents between coplanar electrodes on the films, using the TOF. Due to the columnar growth of the films, this experimental setup allowed the observation of the influence of the grain boundaries on the carrier transport. In our arrangement a 10 μsec white light pulse, produced by a stroboscopic lamp, generates the electron-hole pairs in a region adjacent to one of the aquadag electrodes. The typical interelectrode distance is about 0.8 cm. In order to avoid space-charge effects, neutral density filters were used to control the intensity of the light pulse. The transient photocurrents are amplified by a high-gain wide bandwidth amplifier, and then averaged and recorded by a digital signal analyzer. The experiment was triggered in the manual mode. The number of pulses averaged depended on the signal-to-noise ratio, typically the results presented here represent the average of eight photocurrents measured under the same conditions. In order to avoid the accumulation of space charge in the sample, at the beginning of each record the electrodes were shorted and the sample exposed to several flashes from the lamp.

III. RESULTS AND DISCUSSION

A. Transient transport in CdTe films grown by CSVT

Figure 1(a) shows the typical electron photocurrent decay plotted with linear scales measured at room temperature with an applied bias voltage of 10 V. The photocurrent amplitude is about 0.2 μA and has been normalized to unity. A monotonic decay due to the charge trapping is observed. The transit time, indicated by the arrow, was determined from Fig. 1(b), where the same data as in Fig. 1(a) for an extended time range from 0.1–1000 msec is plotted with log-log scales. In this graph the photocurrent shape can be fitted approximately by two straight lines with different slopes. The arrow indicating

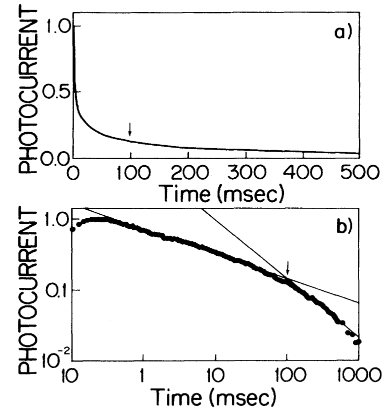

FIG. 1. (a) Linear plot of the electron transient photocurrent in arbitrary units, measured at room temperature and an applied electric field of 10 V/cm. (b) Log-log plot of the same data as in (a), for an extended range of time. In both graphs the arrows indicate the transit time.

the change in the slope determines the transit time. This behavior of the photocurrent can be described by the power-law equation

$$I(t) \sim \begin{cases} t^{-(1-\alpha_1)}, & t \le t_T \\ t^{-(1+\alpha_2)}, & t > t_T \end{cases}, \tag{1}$$

where t_T is the transit time and α_1 and α_2 are parameters related to the slopes of the photocurrent decay. Figure 2 shows five transient photocurrents measured with different applied bias voltages. In this plot the time axis has been normalized to the transit time t_T, and the

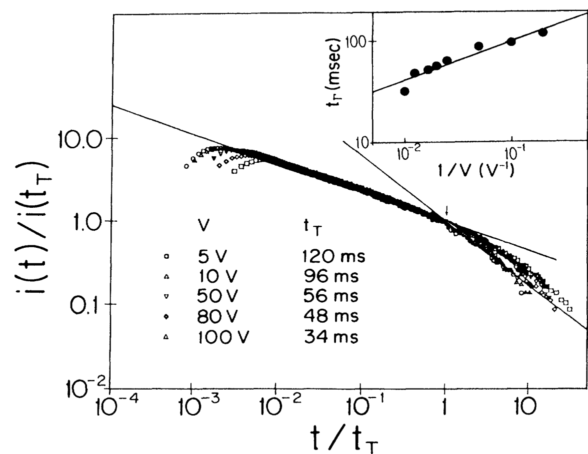

FIG. 2. Superposition of normalized electron transient photocurrents measured at different applied bias voltages. In all the traces, the data are normalized to the transit time and to the corresponding value of the photocurrent at the transit time. The inset shows the log-log plot of the transit time vs the reciprocal of the applied bias voltage.

current axis to the value of the current at the transit time $i(t_T)$. Note that the photocurrent shape remains approximately the same, although the transit time changes by almost one order of magnitude in this range of applied bias voltage. That is, the photocurrent shape in universal.[2] The inset shows the dependence of transit time on the inverse of the applied bias voltage, with log-log scales. The fit to the straight line indicates a transit time dependence on the applied electric field E given by

$$t_T \sim E^{-1/\beta} , \tag{2}$$

where β is a parameter related to the slope of the straight line. The photocurrent dependence on the temperature is shown in Fig. 3. The photocurrents have been normalized to unity and displaced arbitrarily along the current axis. The transit time, indicated by the arrow in each curve, has a thermally activated behavior. This is shown in the inset where the drift mobility is plotted versus $1/kT$. The fit in this figure provides an activation energy for the drift mobility of 0.48 eV.

The experimental results depicted above show that the photocurrent decays with a universal shape and follows a power-law behavior with time. The transit time defined by the change in the slope is not linearly dependent on the reciprocal of the applied bias voltage. The drift mobility is thermally activated and depends on the applied bias voltage. These are the general characteristics of the dispersive transient transport observed in disordered solids like amorphous semiconductors,[3,5,9,10] glasses,[11,12] polymer films,[13,14] etc. In this kind of transport, the photocurrent decay has a power-law behavior given by the Scher and Montroll (SM) equation[2]

$$i(t) \sim \begin{cases} t^{-(1-\alpha)}, & t \le t_T \\ t^{-(1+\alpha)}, & t > t_T \end{cases} . \tag{3}$$

The photocurrent shape given by Eq. (1) deviates from the SM equation in the different values of α for the pre-

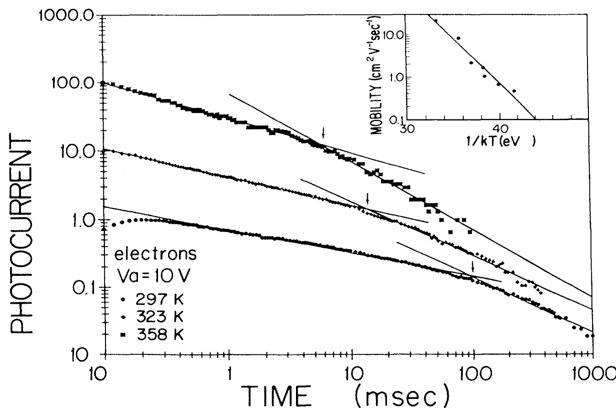

FIG. 3. Electron transient photocurrents, in arbitrary units, measured at different temperatures and an applied electric field of 10 V/cm. The arrow indicates the transit time in each trace. In the inset is shown the exponential behavior of the electron drift mobility vs $1/kT$. The energy of activation given by the fit to the straight line is 0.48 eV.

transit and postransit time branches of the photocurrent. This behavior, commonly observed in other materials,[15,16] can be explained in terms of the multiple-trapping (MT) model by a continuous localized state density having a functional energy dependence different from the exponential one,[15] as would be the case in the SM equation. A protrusion due to a predominant localized state in an exponential density of states can also lead to deviations from the SM equation.[17,18] From the point of view of the SM theory the deviations of Eq. (3) can be due to the variation of the hopping time distributions.[19] Equation (3) follows from a waiting time distribution given by

$$\psi(t) \sim t^{-(1+\alpha)} . \tag{4}$$

The SM equation holds in the time and temperature ranges where Eq. (4) holds; out of these ranges another time distribution must be sought to fit the data. The transit-time behavior given by Eq. (2) agrees with the dispersive transient transport theory.[5] In our case the transit time dependence on $1/V$ is sublinear instead of the supralinear[2] or linear[20] dependences observed in other materials. This is because the value of β given by the fit in the inset of Fig. 2 is greater than one. The activation energy of the drift mobility has been interpreted as being the deepest energy from which the carriers thermalize at the transit time moment.[5] It has also been related to the energy level of a predominant localized state in the band gap of the material.[21] Thus, we can relate our experimental results to an exponential distributions of traps in addition to a trapping center localized at 0.48 eV from the conduction band. From the available experimental data, this distribution lies from 0.50 to 0.53 eV in the forbidden band gap of the films.

The origin of the dispersive behavior observed in the transient transport of disordered materials comes from the wide energy distributions of the localized states which control the transient transport.[22] This condition holds *per se* in disordered materials, but also holds in some crystalline materials which present dispersive transport characteristics.[23,24] In our case, the polycrystalline materials is an intermediate case between crystalline and amorphous material. A great variety of defects are produced at the grain boundaries due to the crystallographic misfit. In addition, the crystalline material in the bulk of the grain can be imperfect. By using other experimental techniques, such as photoluminescence[25,26] and thermal stimulated conductivity,[27] localized defects have been identified having energies from 0.5 to 0.32 eV in this same kind of film. Some of these levels are identified as defects in the bulk material, but some others could lie at the grain boundaries. The electron trapping level at 0.48 eV has not been identified, at least in monocrystalline CdTe, and could be a defect localized at the grain boundaries. In some polycrystalline materials[28] localized centers having an exponential energy distribution are found such as those reported in amorphous materials. In conclusion, the transient transport in CdTe polycrystalline films grown by the CSVT technique presents the general characteristics of dispersive transient transport. This behavior originates from the wide energy distribution of

the trapping centers. We suggest that this distribution is exponential in association with a predominant localized center.

B. Transient transport in CdTe films grown by HWFE

In this kind of film the photocurrent shapes depend remarkably on the distance L between electrodes. In Fig. 4 the transient photocurrents for three different applied bias voltages and varying length L are plotted with linear scales: (a), (b), and (c) correspond to $L=0.50$, 0.85, and 1.3 cm, respectively. For the three lengths, there is a photocurrent peak for which the position in time is not changed by the applied bias voltage and which shifts toward shorter times when the interelectrode distance decreases. The effect of the bias voltage is to increase the photocurrent amplitude linearly. Figure 5 shows the log-log plots of the same data as in Fig. 4 over the extended range from 0.1–1000 msec. For times longer than the photocurrent peak time, the decay follows a power-law behavior and there is no change in the slope indicating a transit time. Thus, this part of the photocurrent trace can be described by the first branch of Eq. (1). It can also be observed that the slope of the decay does not change appreciably with the applied bias voltage and increases slightly with the interelectrode distance. The lack of dependence of the slope decay on bias voltage indicates that the photocurrent shape is universal, as in the films grown by the CSVT technique. In this case the post-transit time branch of the photocurrent lies beyond the measurement range. The temperature variation produces a strong change in the photocurrent shape. In Fig. 6 several current traces measured at different temperatures from 375–403 K are plotted, an interelectrode distance of 0.85 cm and a bias voltage of 500 V. The photocurrent peak shifts notably toward shorter times when temperature is increased. In the inset is shown the temperature dependence of the reciprocal of photocurrent peak time. This time is a thermally activated quantity, with an activation energy of 0.49 eV, as shown by fitting to the straight line. This means that the time position of the photocurrent peak behaves proportionally to a release time from a trapping center, localized at 0.49 eV from the bottom of the conduction band. We found the same dependence on temperature of the photocurrent traces for the three different interelectrode distances used, with the same activation energy. This is evidence that the peak originates from the same kind of trapping centers in the three cases. Photocurrent traces similar to that of Fig. 4 have been reported for other materials.[9,29] The photocurrent peak has been explained in terms of space-charge limited currents and related to a transit time. In our case the time position of the photocurrent peak does not shift with the applied bias voltage, so it is not a transit time. In addition, we performed experiments with different light pulse intensities. The photocurrent traces of these experiments are shown in Fig. 7. It can be seen that the photocurrent peak does not shift with the variation of the light intensity, as expected in the space-charge limited current case. The plot verifies that the photocurrent peak observed in Fig. 4 is not a space-charge effect.

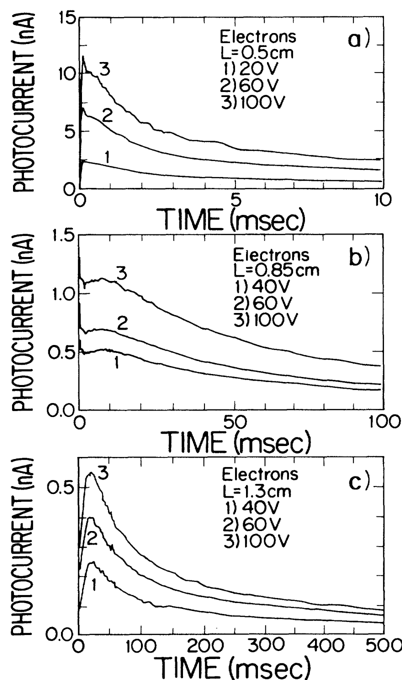

FIG. 4. Linear plots of electron transient photocurrents measured at three different voltages at room temperature for three values of the interelectrode distance (a), (b), and (c) correspond to 0.5, 0.85, and 1.3 cm, respectively. Note the different range in the time axis for each plot.

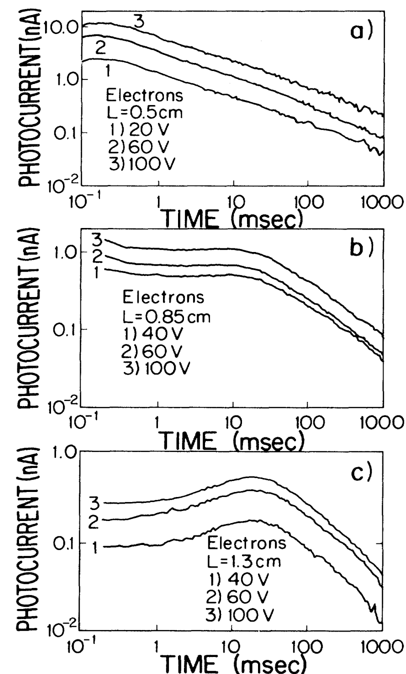

FIG. 5. Log-log plot of the data in Fig. 4 in the extended time range 0.1–1000 msec. (a), (b), and (c) correspond to the interelectrode distances 0.5, 0.85, and 1.3 cm, respectively.

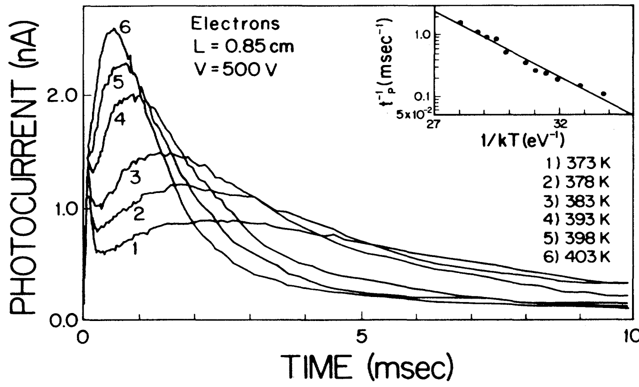

FIG. 6. Electron transient photocurrents measured at different temperatures with an applied electric field of 590 V/cm. The inset shows the dependence on $1/kT$ of the reciprocal of the photocurrent peak time t_p^{-1}. The activation energy obtained from the fit is 0.49 eV.

At long times after the photocurrent peak, the behavior of the transient transport observed in the films grown by the HWFE technique is similar to the transport depicted in the previous section. The pretransit time branch of the photocurrent has a power-law behavior with universal shape. The inability to determine a transit time from the photocurrent traces shows that deep trapping and recombination processes are more important in these films than in those grown by the CSVT technique. This may be due to the larger number of grain boundaries which electrons must cross in the smaller-grain-size films. These results indicate that deep trapping and recombination of charge take place mainly at the grain boundaries of the material. However, the defects in the crystalline material of the grain bulk can also influence these processes. At present we do not have information about the

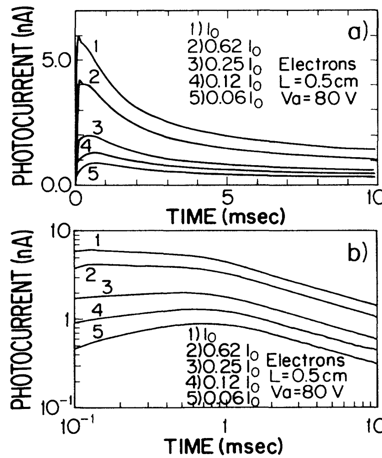

FIG. 7. (a) Linear plots of the electron transient photocurrents measured at different light pulse intensities and an applied electric field of 160 V/cm. I_o is the light pulse intensity commonly used in these experiments. (b) Log-log plots of the same data as in (a).

perfection of the grain bulk, but we suppose that it should be similar in both kinds of films, and thus, the difference observed in the experimental results is due mainly to the different number of grain boundaries per unit length in the films.

These results also show a strong influence of a localized trapping center. The thermal release of charge from this center, previously filled by the light pulse, along with the recombination of charge, causes the photocurrent peak. In a previous paper[7] we found that the multiple-trapping model with a single trapping level, considering the recombination of charge, appropriately reproduces the shape of the photocurrent peak. The fundamental equations of this model are[30,31,32] as follows. The equation for the current density $J(t)$,

$$J(t)=\int_0^1 n(x,t)E(x,t)dx \;, \tag{5}$$

Poisson's equation for the electrical field $E(x,t)$,

$$\frac{\partial E(x,t)}{\partial x}=n(x,t)+n_t(x,t)-n_r(x,t) \;, \tag{6}$$

and the charge balance equation for the single trapping level, characterized by a trapping time τ and a release time τ_d,

$$\frac{\partial n_t}{\partial t}=\frac{n}{\tau}-\frac{n_t}{\tau_d} \;. \tag{7}$$

In these equations, $n(x,t)$ is the free charge in the conduction band, $n_t(x,t)$ is the trapped charge, and $n_r(x,t)$ is the charge lost by recombination. This charge is being neutralized during the recombination process and will not contribute to the electrical field. Furthermore, it will be assumed that $n_r(x,t)$ is given by

$$n_r(x,t)=n_{ro}(x)\exp\left[-\frac{t}{\tau'}\right] \;, \tag{8}$$

where τ' is a decay time characteristic of this trapping. In addition, the above equations have been simplified by normalizing to unity the charge and drift mobility of the electron, the interelectrode distance, and the transversal area for the transport. Assuming that the photogenerated charge is too small to modify the applied electric field, which corresponds to the "small signal" case,[33] these equations can be solved in an analytical way, and it is found that the photocurrent shape, given by the solution for $J(t)$, is

$$J(t)=\frac{J_o\theta}{1+\theta}+\frac{\beta\Delta\theta}{1+\Delta\theta}\left[1-\Theta\exp\left[-(1+\Delta\theta)\frac{t}{\tau}\right]\right] \times\exp\left[-\frac{t}{\tau'}\right] \;, \tag{9}$$

where

$$\Theta=1+\frac{J_o\theta(1+\Delta\theta)}{\beta\Delta\theta(1+\theta)} \;, \tag{10a}$$

$$\beta=\int_0^1 n_{ro}(x)E(x,0)dx, \quad \theta=\frac{\tau}{\tau_d} \;, \quad \theta'=\frac{\tau}{\tau'}, \quad \Delta\theta=\theta-\theta' \;. \tag{10b}$$

In the solution of these equations it was assumed $J(0)=0$. The photocurrent is then caused by the charge released from the traps previously filled by the light pulse. Thus, J_o is a quantity related to the initial distributions of n, n_t, and n_r, and to the applied bias voltage.

In Fig. 8 the fit of Eq. (9) to the experimental data is shown. Figures 8(a), 8(b), and 8(c) correspond to each of the three interelectrode distances and the bias voltage is the same in the three cases. A good agreement between the model and the experimental data is seen. The parameter τ_d was kept fixed in Eq. (9), and the fit provided the values of τ and τ' shown in this figure for the three cases. An increase in these trappings times is observed as the interelectrode distance is increased. The value of τ_d is 10 msec, which corresponds to the release time from a trapping center localized at 0.49 eV from the conduction band with an escape-attempt frequency of 10^{10} sec^{-1}. Furthermore, Eq. (9) predicts a time position of the photocurrent peak as

$$t_p^{-1} \sim \tau^{-1} + \tau_d^{-1} - \tau'^{-1} . \tag{11}$$

From this equation it can been seen that the temperature dependence of the peak time t_p is proportional to the exponential temperature dependence of the release time τ_d, due to the weak dependences of the trapping times τ and τ'.[1] Thus the shift of the photocurrent peak with the temperature is also explained by this simple model.

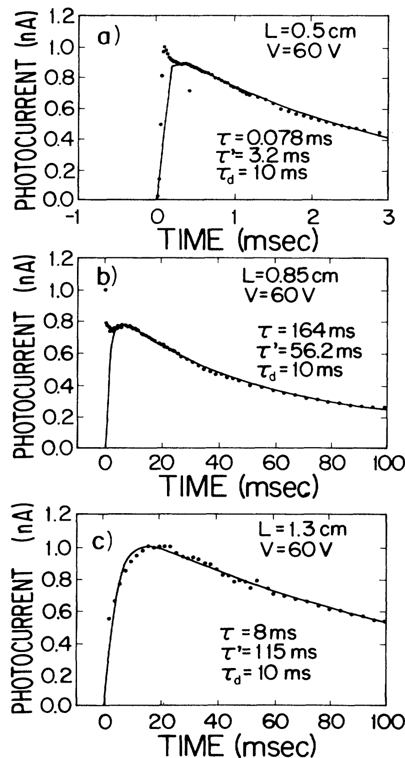

FIG. 8. Fit of the experimental data to Eq. (9). The solid circles correspond to experimental points and the solid line to the theoretical curve. (a), (b), and (c) correspond to the interelectrode distances 0.5, 0.85, and 1.3 cm, respectively. The fit provides the values of the parameters τ and τ' in each case.

From this model, the shift of the photocurrent peak with the interelectrode distance is due to the increase of the characteristic times τ and τ', which in principle are independent of this length. So, this shift should be attributed to a feature not considered in the model. An important phenomenon could be the trapping at the surface. According to some authors,[34] surface trapping is equivalent to a delay in the photogeneration of charge carriers.

In conclusion, the electron transient transport observed in the CdTe films grown by the HWFE technique is dispersive with a universal shape for the pretransit branch of the photocurrents. This shows the influence of the wide energy distribution of the localized trapping centers in the films. The recombination and deep trapping of charge at the grain boundaries do not allow the determination of a transit time in the photocurrent traces. The photocurrent peak is explained by the presence of a localized trapping center at 0.49 eV in the band gap of the films. The thermal release of charge from this trap, along with the subsequent recombination of charge, causes the photocurrent peak as predicted by the proposed simple model. This trapping center may be the same as that observed in the films grown by the CSVT technique. The influence of this trap on the transient transport of the films indicates that its concentration per unit volume is much greater in the films grown by the HWFE technique.

C. Transient transport in CdTe films grown by rf sputtering

The transient photocurrents measured in this kind of film show evidences of severe trapping events, yielding a

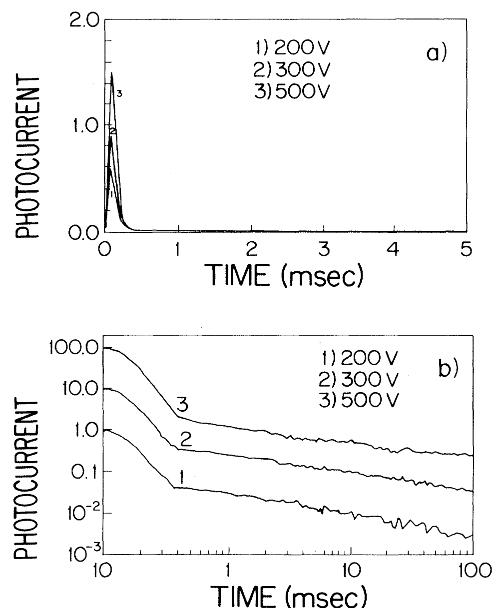

FIG. 9. (a) Electron transient photocurrents, in arbitrary units, measured at room temperature with three different applied bias voltages, plotted on linear scales. (b) The same data as in (a), plotted on log-log scales for the extended time range 0.1 – 1000 msec.

fast decay of the photocurrent as shown in Fig. 9(a). In this figure three photocurrent pulses measured with three different voltages at room temperature are plotted with linear scales. When these data are plotted with log-log scales, the fast decay appears as a peak and a power-law behavior can be seen for longer times, as observed in the log-log plots of Fig. 9(b). The slope of the straight line is voltage independent and there are no changes of slope in the decay which could indicate a transit time. The temperature variation does not change the shape of the photocurrents over a wide range. These results show that deep trapping and recombination of charge control the transport in these films causing the fast photocurrent decay and the inability to determine a transit time. Only the photocurrent amplitude varies when voltage and temperature change.

Like the films grown by the HWFE technique, these films have a small grain size, and so electrons encounter a great number of grain boundaries along the path between electrodes. Thus we can relate the deep trapping and recombination of charge to phenomena taking place at the grain boundaries. In this case there is no predominant localized state which could trap and release charge to cause a photocurrent peak, as in the case of the films grown by the HWFE technique. In conclusion, these results show that transient transport in these films is dominated by the deep trapping and recombination of charge.

ACKNOWLEDGMENTS

We acknowledge the help of M. Becerril for his assistance in sample preparation. This work was partially supported by Consejo Nacional de Ciencia y Tecnología (CONACyT-México).

[1]M. Martini, J. W. Mayer, and K. R. Zanio, in *Applied Solid State Science,* edited by R. Wolfe (Academic, New York, 1978), Vol. 3, p. 181.

[2]H. Scher and E. W. Montroll, Phys. Rev. B **12**, 2245 (1975).

[3]G. Pfister and H. Scher, Phys. Rev. B **15**, 2062 (1977).

[4]J. M. Marshall, Rep. Prog. Phys. **46**, 1235 (1983).

[5]T. Tiedje, in *Semiconductors and Semimetals,* edited by R. K. Willardson and A. C. Beer (Academic, New York, 1984), Vol. 21, Pt. C, Chap. 6, p. 207.

[6]R. Ramíez-Bon, F. Sánchez-Sinencio, G. González de la Cruz, and O. Zelaya, Solid State Commun. **80**, 427 (1991).

[7]R. Ramírez-Bon, F. Sánchez-Sinencio, G. González de la Cruz, and O. Zelaya, Solid State Commun. **85**, 15 (1993).

[8]Lawrence L. Kasmerzki, in *Polycrystalline and Amorphous Thin Films,* edited by Lawrence L. Kasmerzki (Academic, New York, 1980), Chap. 3, p. 59.

[9]T. Tiedje, B. Abeles, D. L. Morel, T. D. Moustakas, and C. R. Wronsky, Appl. Phys. Lett. **36**, 695 (1980).

[10]T. Tiedje, J. M. Cebulka, D. L. Morel, and B. Abeles, Phys. Rev. Lett. **46**, 1425 (1981).

[11]M. D. Tabak, Phys. Rev. B **2**, 2104 (1970).

[12]M. E. Scharfe, Phys. Rev. B **2**, 5025 (1970).

[13]G. Pfister and C. H. Griffiths, Phys. Rev. Lett. **40**, 659 (1987).

[14]F. C. Boss and D. M. Burland, Phys. Rev. Lett. **58**, 152 (1987).

[15]J. M. Marshall, H. Michiel, and G. J. Adriaenssens, Philos. Mag. B **47**, 211 (1983).

[16]J. M. Marshall, H. Michiel, and G. J. Adriaenssens, Philos. Mag. B **48**, 187 (1983).

[17]J. M. Marshall and R. A. Street, Solid State Commun. **50** 91 (1984).

[18]G. Seynhaeve, G. J. Adriaenssens, and H. Michiel, Solid State Commun. **56**, 323 (1985).

[19]G. Pfister and H. Scher, Adv. Phys. **27**, 747 (1978).

[20]P. B. Kirby and W. Paul, Phys. Rev. B **25**, 5373 (1982).

[21]W. E. Spear, D. Allan, P. G. LeComber, and A. Ghaith, Philos. Mag. B **41**, 419 (1980).

[22]J. Orenstein, M. A. Kastner, and V. Vaninov, Philos. Mag. B **46**, 23 (1982).

[23]J. M. Marshall, J. Phys. C **10**, 1283 (1977).

[24]J. B. Webb, D. F. Williams, and J. Noolandi, Solid State Commun. **31**, 905 (1979).

[25]J. M. Figueroa, F. Sánchez-Sinencio, J. G. Mendoza-Alvarez, O. Zelaya, C. Vazquez-López, and J. S. Helman, J. Appl. Phys. **60**, 452 (1986).

[26]J. M. Figueroa, F. Sánchez-Sinencio, J. G. Mendoza-Alvarez, O. Zelaya, G. Contreras-Puente, and A. Díaz-Góngora, J. Cryst. Growth **106**, 651 (1989).

[27]R. Ramirez-Bon, F. J. Espinoza-Beltrán, H. Arizpe-Chávez, F. Sánchez-Sinencio, and O. Zelaya, Superficies y Vacío (Mexico) **2**, 94 (1990).

[28]J. Werner and M. Peisl, Phys. Rev. B **31**, 6881 (1985).

[29]W. D. Gill, J. Appl. Phys. **43**, 5033 (1972).

[30]F. W. Schmidlin, Solid State Commun. **22**, 451 (1977).

[31]F. W. Schmidlin, Phys. Rev. B **16**, 2362 (1977).

[32]J. Noolandi, Phys. Rev. B **16**, 4466 (1977).

[33]R. M. Blakney and H. P. Grunwald, Phys. Rev. **159**, 658 (1967).

[34]M. Silver, K. S. Dy, and I. L. Huang, Phys. Rev. Lett. **27**, 21 (1971).